Raising the Standard of Specimen Preparation for Aberration-Corrected TEM and STEM

R. R. Cerchiara,[1] * P. E. Fischione,[1] J. Liu,[1] J. M Matesa,[1] A. C. Robins,[1] H. L. Fraser,[2] and A. Genc[2]

[1] E. A. Fischione Instruments, Inc., 9003 Corporate Circle, Export, PA 15632

[2] The Ohio State University, Columbus, OH 43210

* rr_cerchiara@fischione.com

https://doi.org/10.1017/S1551929510001197 Published online by Cambridge University Press

Introduction

With the recent advances made in monochromation of electron sources and Cs-correction, the point resolution of the transmission electron microscope (TEM) has been extended into the sub-Angstrom regime. This development has led to an important consequence—that specimen preparation has become a more critical issue for the materials scientist. Nanoscale artifacts that could be tolerated a few years ago when imaging in the 0.1–0.15 nm range can no longer be allowed. An example is hydrocarbon contamination, which although only a few monolayers thick, obscures the area of interest [1]. Other examples include residual deformation and oxidation following traditional mechanical methods. Ion-based methods may induce amorphization and implantation defects, depending on the type of ion, its energy, and the particular protocol that is used.

Specimen preparation begins with the application of either a conventional or focused ion beam (FIB) and ends with post-processing to optimize the results. In the FIB, a Ga liquid metal ion source is operated at accelerating voltages ranging from 30 keV to 1 keV. Depending on the beam size and current, this tool can be used to either cut or polish a cross section of the desired material. Cryogenic specimen stages have been added to allow treatment of polymers as well as metals or ceramics. Most commercial instruments have combined an electron column with the ion column, permitting high-resolution imaging with secondary or backscattered electrons during or after FIB. A variety of specimen preparation techniques and configurations are available, including *ex-* and *in-situ* lift-outs and the H-Bar [2].

Specimen Quality Enhancement

The NanoMilling^{SM} process, as a complementary technique to FIB, has been demonstrated for *in-situ* lift-out samples of ceramics and certain metallic alloys [3, 4]. Damaged layers (0.5–2 nm thick) may remain after FIB milling with 2–5 keV Ga ions [5]. These layers contain amorphous specimen material and implanted Ga ions, with the distribution dependent on the specimen material and preparation protocol. Unless the damaged layer thickness can be reduced or eliminated, nonuniform ("mottled") contrast will be observed during imaging in the TEM.

The damaged layer is removed in the Model 1040 NanoMill® TEM specimen preparation system without altering the specimen chemistry or crystalline structure. Redeposition during ion milling is minimized by careful orientation of the ion beam with respect to the lamella attached to its support grid (Figure 1). Typical lamella dimensions are ~5 µm × 10 µm × 100 nm. Because the lamella and ion beam are of the same relative size, there is no contact of Ar ions or neutral species with the support grid. Imaging occurs as the ion-induced electrons released during the sputtering process are collected by the secondary electron detector (SED). Once an image is scanned, the area of interest may be selected and the final ion milling protocol can be executed (Figure 2). A concentrated Ar ion beam (50–2000 eV) of 2–4 µm diameter is directed at low incident angles (0 to ±10°) to a lamella maintained at a temperature between 25° and –175°C.

Results

Figure 3 shows milling rate data extracted from atomic force microscopy (AFM) measurements made of trenches ion milled into silicon. Ion milling rates vary as a function of the specimen material and instrument parameters. For the present case, Figure 3 shows that the ion milling rate increased as a function of ion source voltage to a maximum of 7.7 nm/min. Improvements in 200 keV HRTEM image quality were observed for Si specimens that received final milling with 200-eV Ar ions after initial thinning in the FIB at 30 keV (Figure 4) [6]. Atomic resolution imaging of the dumbbell structure was possible (Figure 4) [7].

Post-FIB processing provides a significant improvement in image contrast for various metallic alloys, including multi-phase microstructures that are environmentally sensitive. This

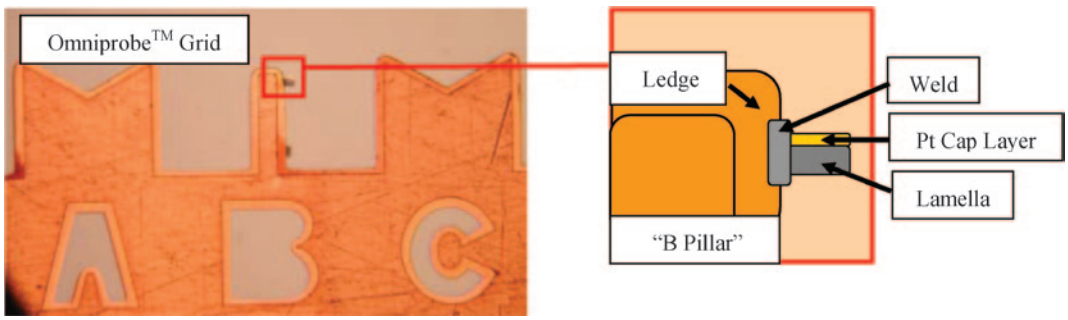

Figure 1: Optical micrograph (left) and schematic (right) of *in situ* lift-out specimen.

 doi:10.1017/S1551929510001197

https://doi.org/10.1017/S1551929510001197 Published online by Cambridge University Press

Model 1040 NanoMill®

TEM specimen preparation system

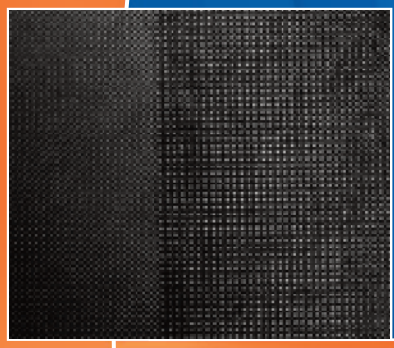

Revolutionary ultra-low-energy, inert gas, concentrated ion beam produces specimens with no amorphous damage or implanted layers

Fischione's NanoMill® system is an excellent tool for creating the high-quality, thin specimens needed for advanced transmission electron microscopy (TEM) imaging and analysis. It is ideal for both post-FIB (focused ion beam) processing and enhancing conventionally prepared specimens.

Features

- **Ion energies as low as 50eV and up to 2,000eV**
- **Secondary electron detector (SED) imaging for precise milling of a selected area of interest**
- **Removes damaged layers without redeposition**
- **Small diameter argon ion beam (down to 1 micron) with beam scanning capabilities**

Nb:$SrTiO_3$/$SrRuO_3$ specimen prepared by the NanoMilling℠ process and imaged with the TEAM 0.5 at 80kV
Courtesy of Joachim Mayer, Ernst-Ruska Centre, Juelich, Germany and Christian Kisielowski, LBL/NCEM U.S.A.

The NanoMill® System is the subject of United States Patent Nos. 7,132,673 and 7,504,623. Other patents pending.
NanoMill® is a registered trademark of E.A. Fischione Instruments, Inc.

FISCHIONE INSTRUMENTS

EXCELLENCE...MAGNIFIED

9003 Corporate Circle, Export, PA 15632 USA • Tel: 1.724.325.5444 • www.fischione.com

https://doi.org/10.1017/S1551929510001197 Published online by Cambridge University Press

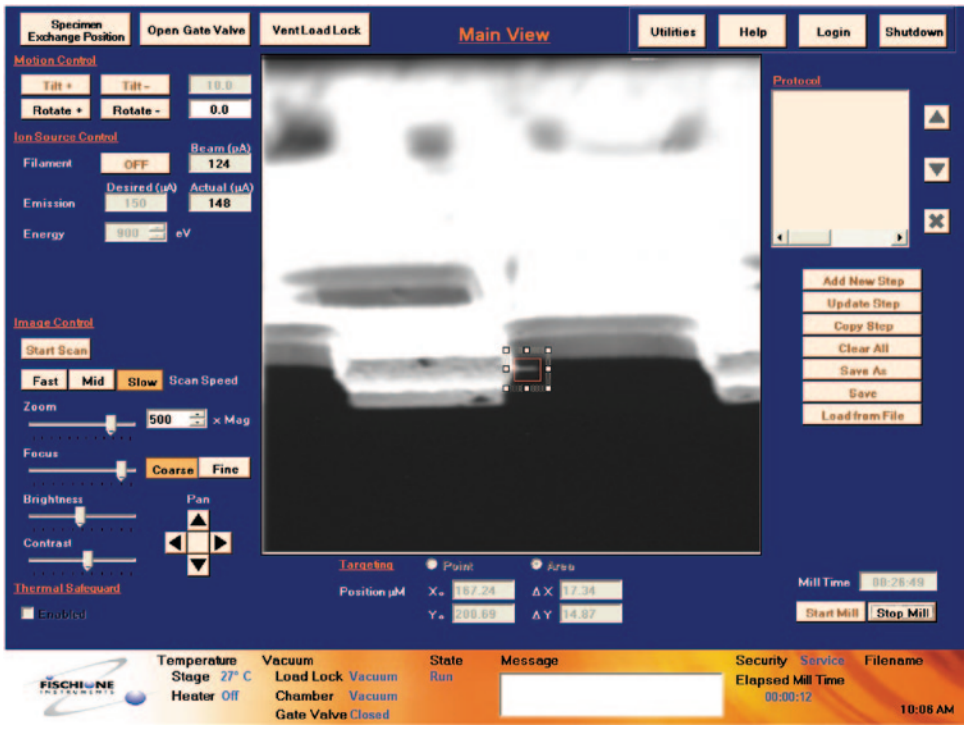

Figure 2: 900 eV secondary electron image of a lamella acquired at 10° stage tilt.

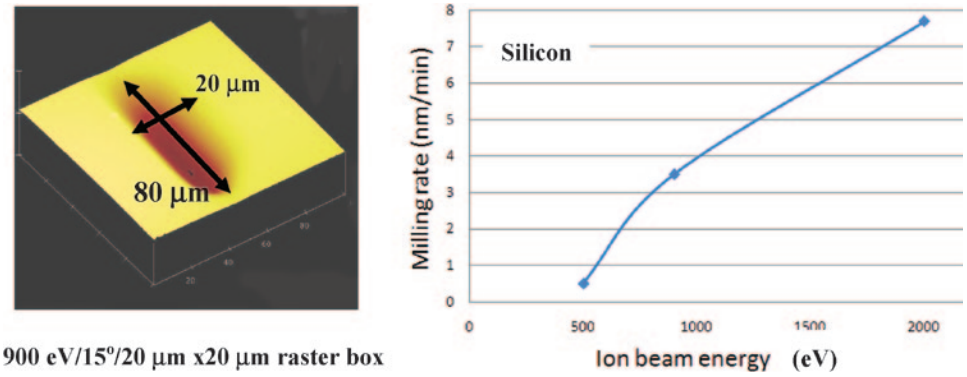

Figure 3: AFM image of an ion milled trench (left) and milling rate data versus beam energy (right) for silicon.

was demonstrated in the case of the conventionally ion-milled titanium alloy depicted in Figure 5. After foil perforation, the edge had a 10-nm-wide amorphous rim. Further thinning with a low-voltage, concentrated Ar ion beam resulted in total removal of this damaged zone. Lattice fringes were found to terminate at the edge of the perforation.

Improvements also have been observed for ceramics, specifically titanates based on strontium and barium. These crystals are highly ordered and contain interpenetrating lattices populated by ions that are low in atomic number. Aberration-corrected, high-angle annular dark field (HAADF) STEM is often used to analyze these materials at high resolution. Images of a $SrTiO_3$ specimen after FIB and subsequent concentrated Ar ion milling are shown in Figure 6. The initial mottled contrast was reduced so that the ion positions could be located with confidence.

Layered microstructures are difficult to prepare by any ion-based technique. Intermixing of the individual layers may occur, and the interfaces that separate them may become indistinct. An example of this effect is shown in Figure 7, where no obvious demarcation exists between $BaTiO_3$ and $SrTiO_3$ after FIB milling [8]. Following a NanoMilling^{SM} process, the positions of the ions, as well as the

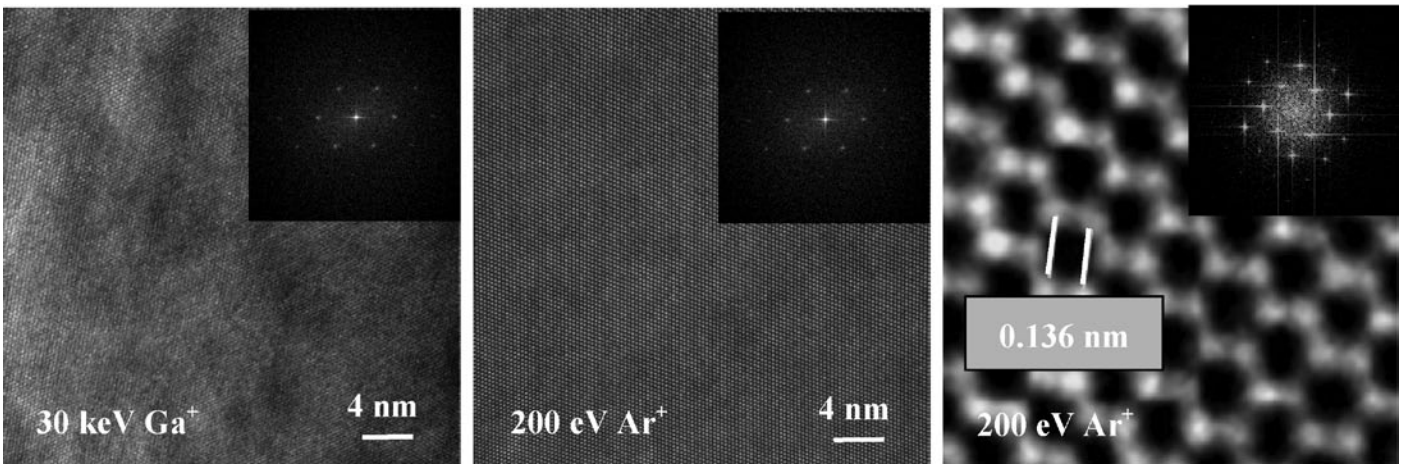

Figure 4: Uncorrected HRTEM images of silicon after 30 keV FIB (left) and subsequent 200 eV post-FIB processing (center). Aberration-corrected image (right) showing dumbbell structure. The FFT of the lattice image includes higher periodicities evident after the Ga implanted and amorphized layers were removed.

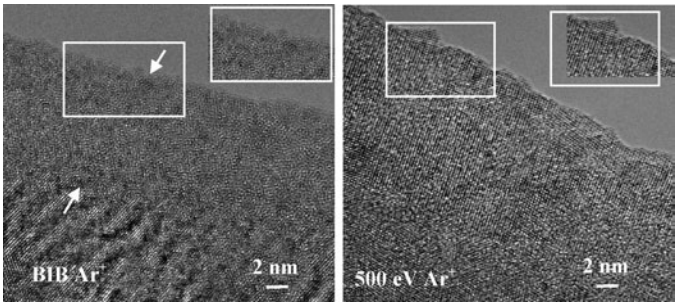

Figure 5: Uncorrected HRTEM images of a titanium alloy after conventional ion milling (left) and 500 eV post-processing (right). The 10–12 nm wide amorphous rim indicated by the double arrows was removed, with lattice extending to the perforation.

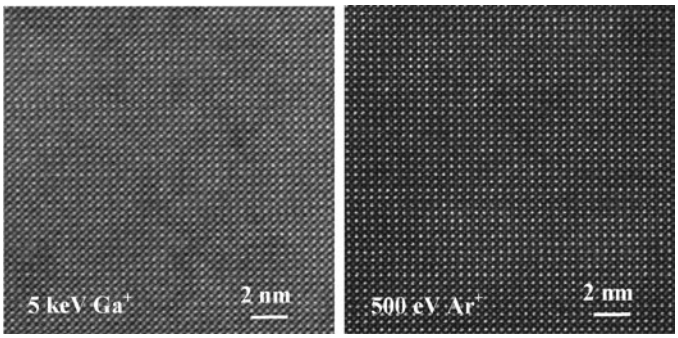

Figure 6: Aberration-corrected HAADF STEM images of $SrTiO_3$ after 5 keV FIB (left) and subsequent 500 eV post-FIB processing (right). The mottled contrast was significantly reduced.

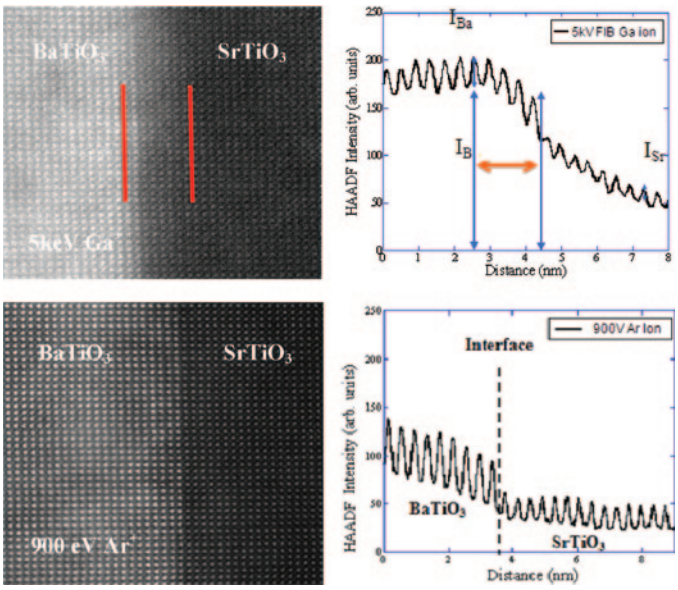

Figure 7: Aberration-corrected HAADF STEM images of $BaTiO_3/SrTiO_3$ after 5 keV FIB (upper left) and subsequent 900 eV post-FIB processing (lower left). The positions of the ions and interphase interface are found in the respective image intensity profiles.

interphase interface, can be readily established. The former corresponds with the local maxima in the intensity versus distance profile, and the latter corresponds to the sharp transition in the data.

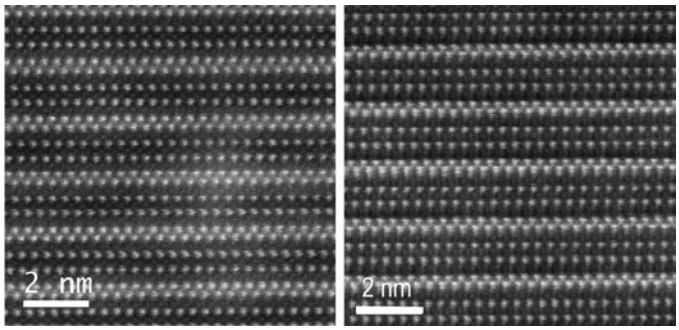

Figure 8: 200 keV HAADF STEM lattice images taken from a $Bi_4Ti_3O_{12}$ lamella after 2 keV FIB (left) and subsequent 700 eV post-FIB processing of an H-Bar (right).

This process is currently being extended to other specimen configurations, including the H-Bar. Depending on the dimensions of the FIB box, rastering of the ion beam within its confined space is possible without incurring significant redeposition from the sidewalls. Results of milling a $Bi_4Ti_3O_{12}$ single crystal lamella at near 0° incidence are shown in Figure 8 [9]. The mottled contrast (streaking) remaining after FIB (2 keV) was removed and the image quality was improved.

Conclusions

For accurate TEM and STEM imaging of materials systems on the atomic scale, artifacts must be reduced to the absolute minimum. A higher standard in TEM specimen preparation is achieved by complementing conventional and FIB milling with concentrated, ultra-low-energy Ar ion beam processing.

References

[1] TC Isabell et al., *Microsc Microanal* 5 (1999) 126–35.
[2] LA Giannuzzi, *Introduction to Focused Ion Beams*, Springer, New York, 2005.
[3] PE Fischione et al., Presentation CL4, FEMMS, Kasteel Vaalsbroek, Holland, 2005.
[4] A Genc et al., *Microsc Microanal* 13 (Suppl. 2) (2007), 1520–21.
[5] LA Giannuzzi et al., *Microsc Microanal* 11 (Suppl. 2) (2005) 828–29.
[6] Uncorrected images shown in Figure 4 courtesy of P Midgley, D Cooper, and RE Dunin-Borkowski, University of Cambridge, U.K.
[7] Corrected image shown in Figure 4 courtesy of A Kirkland and C Hetherington, University of Oxford, U.K.
[8] The data and images presented in Figure 7 to appear in A Genc, REA Williams, DE Huber, AW Johnson, HL Fraser, and PE Fischione, "Characterization of FIB Induced Damage in Transmission Electron Microscopy Sample Preparation" in *Ultramicroscopy*.
[9] Images courtesy of K Kisslinger, Brookhaven National Laboratories, Upton, NY.

NanoMill® is a registered trademark of E.A. Fischione Instruments, Inc.

The NanoMill® System is the subject of U.S. Patent Nos. 7,132,673 and 7,504,623. Other patents pending.

MT

https://doi.org/10.1017/S1551929510001197 Published online by Cambridge University Press